Electronic Supplementary Material (ESI) for ChemComm.

Supporting Information for

One-Pot Synthesis of Copper-Nickel Sulfide Nanowires for Overall Water Splitting in Alkaline Media

Dong Cao[a] and Daojian Cheng*[a]

[a] State Key Laboratory of Organic-Inorganic Composites, Beijing University of Chemical Technology, Beijing 100029, People's Republic of China

*Corresponding Author. Email:

chengdj@mail.buct.edu.cn

Experimental section

Chemicals

Oleylamine (OAm, 80-90%), Bis(2,4-pentanedionato) copper(II) ($Cu(acac)_2$, 98%), Nickel chloride hexahydrate ($NiCl_2•6H_2O$, 98%), Dimethyldioctadecylammonium chloride (DDAC, 97%) were all purchased from aladdin industries Inc.. Besides, sulfur powder (S) was purchased from Beijing Chemical Works. Ethanol (C_2H_5OH, 99.7%) and n-hexane (>95%) were also obtained from Beijing Chemical Works. No purification treatment was applied for all the chemicals. The water (18 MΩ cm^{-1}) was obtained from an ultra-pure purification system.

Synthesis of catalysts

In a facile process to synthesize copper-nickel sulfide nanowires, 0.8 mmol cupric (II) acetylacetonate (Aladdin Industrial Inc., 98%), 0.25 mmol nickel (II) chloride hexahydrate (Aladdin Industrial Inc., 99.3%), 0.51 mmol dimethyldistearylammonium chloride (Aladdin Industrial Inc., 97%) were added into a three-necked bottle. Then, 8.5 mL oleylamine (Aladdin Industrial Inc., 80-90%) was put in the same three-necked bottle. Next, these chemicals were mixed under the N_2 atomosphere at 80 ℃ for 45 min. After that, the temperature was raised to 180 ℃ for 4 h. Then, the temperature was raised to 225 ℃ for 1.5 h. Afterward, 0.25 mmol sulfur powder (Aladdin Industrial Inc., 99.5%) was added into the above bottle when the temperature decreased from 225 ℃ to 100 ℃. Subsequently, the temperature was kept at 150 ℃ for 3 h. Finally, the obtained copper-nickel sulfide nanowires were washed

with the mixed solvent of ethanol (Beijing Chemical Works) and hexane (Beijing Chemical Work) for three times. The synthesis of Cu and CuNi nanowires was the same as the method of copper-nickel sulfide nanowires, except temperature was raised to 225 ℃ for 1.5 h and sulfur powder was added into the bottle, respectively.

Electrochemical measurements

The electrochemical performances for both HER and OER were measured in a three-electrode system by a CHI 760E work station (Chen Hua in China). 4 mg of copper-nickel sulfide nanowire was mixed with 0.5 ml ethanol, 0.1 mL water and 15 μL nafion. Then, the catalyst ink was obtained after ultrasound the mixture above for 30 minutes. Meanwhile, a carbon rod and saturated calomel electrode (SCE) were used as the counter electrode and reference electrode, respectively. Beside, 0.2 mL ink of catalyst was dropped on the carbon paper, serving as a working electrode. IR drop was compensated at 95% through positive feedback using the CHI 760E work station. Additionally, the scan rate of CV and LSV were 50 mV s^{-1} and 5 mV s^{-1}, respectively. Furthermore, the electrochemical impedance spectroscopy (EIS) was tested at scanning frequency from 100 kHz to 0.01 Hz.

Characterization of Materials

The morphology and structure of nanomaterials were observed on HT7700 transmission electron microscope and TF20 transmission electron microscope (Jeol 2100F) which is coupled with energy dispersive X-ray spectroscopy (EDS) with an acceleration voltage of 200 kV. In addition, EDS line-scan, selected area electron diffraction (SAED) and mapping analysis were also carried out on a TF20 (Jeol

2100F) with a high-angle annular dark-field scanning transmission electron microscope (HAADF-STEM). The X-ray diffraction (XRD) was recorded on X'Pert PRO MPD (D8) instrument to detect the phase composition of samples. The surface characteristics of materials were tested by X-ray photoelectron spectroscopy (XPS) carried out on ESCALAB 250 XI system with an Mg-Ka source.

Table of content

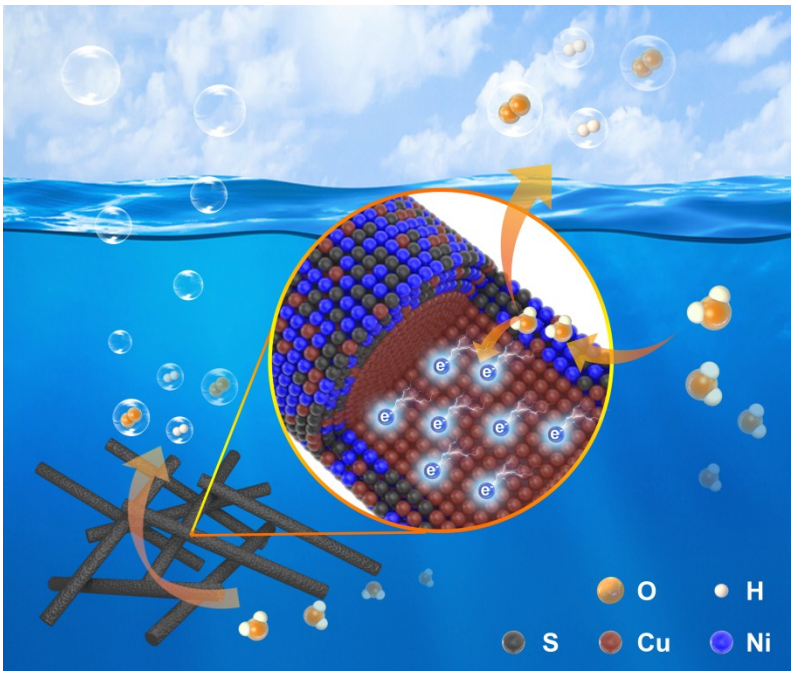

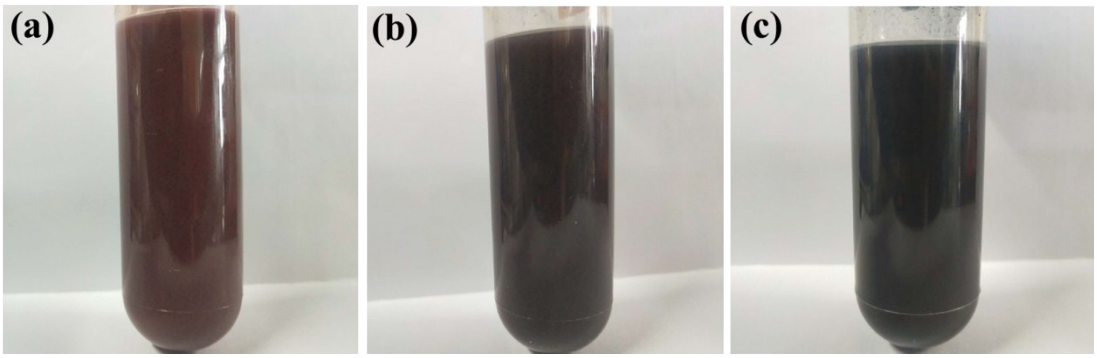

Fig. S1 Photos of different nanocrystals (a) Cu NWs, (b) CuNi NWs and (c) copper-nickel sulfide nanowires.

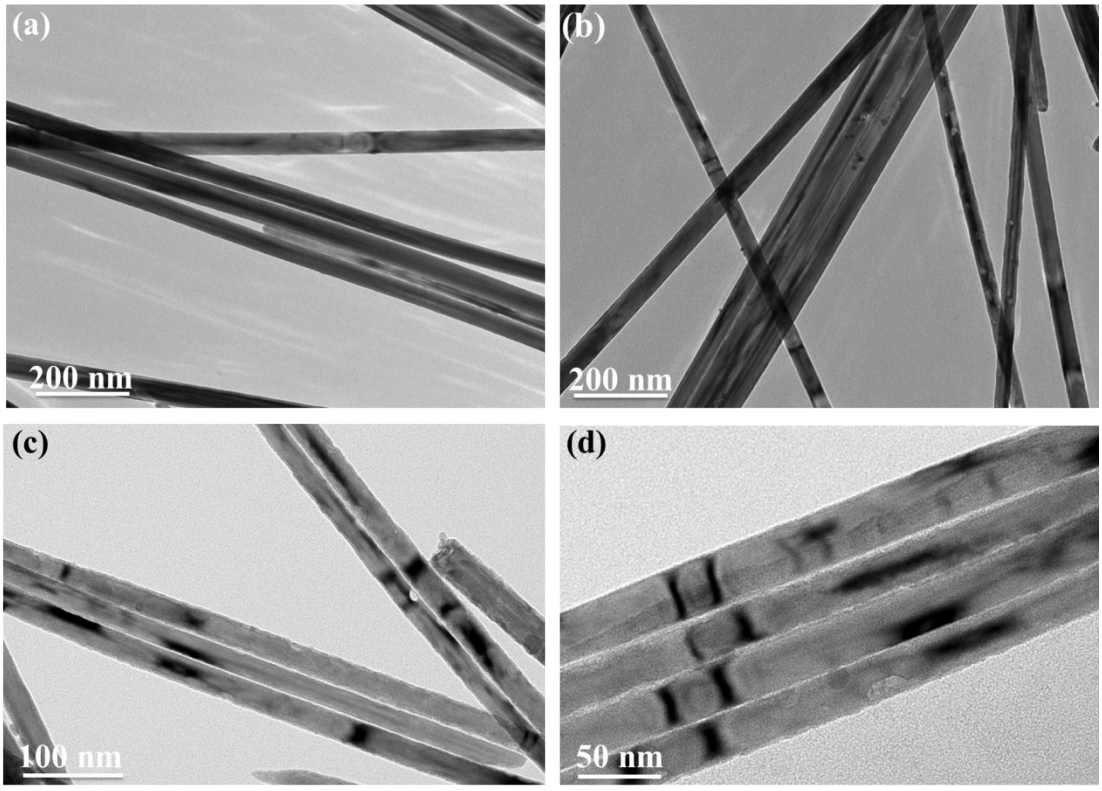

Fig. S2 The TEM images of (a) Cu NWs, (b) CuNi NWs and (c, d) copper-nickel sulfide nanowires.

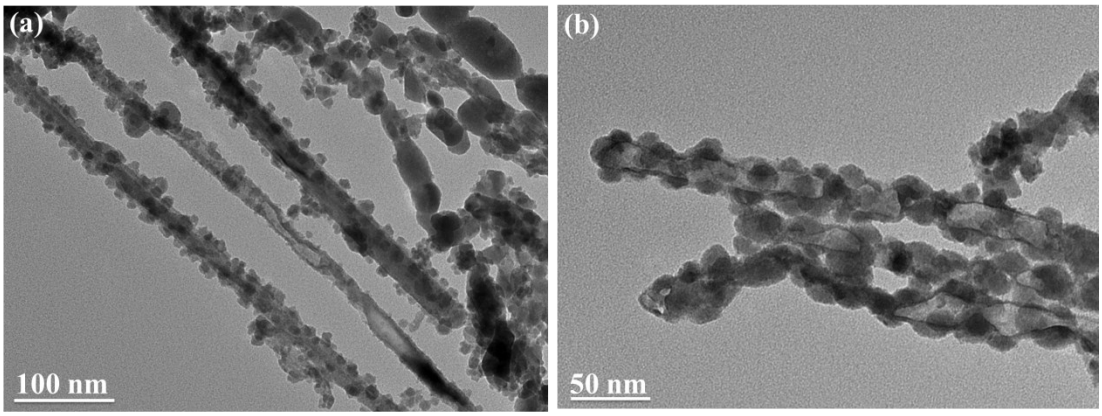

Fig. S3 (a, b) The TEM images of copper sulfide nanocrystals.

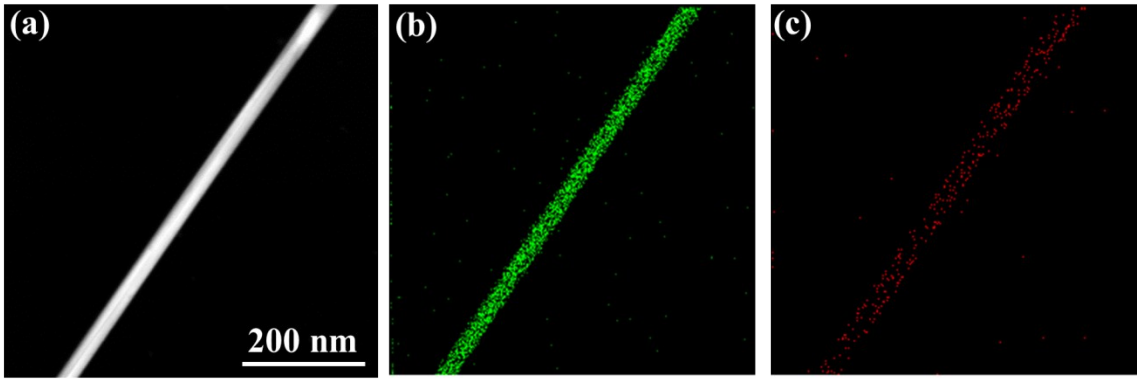

Fig. S4 The element mapping of CuNi alloy NWs. (a) The STEM image, (b) Cu element and (c) Ni element.

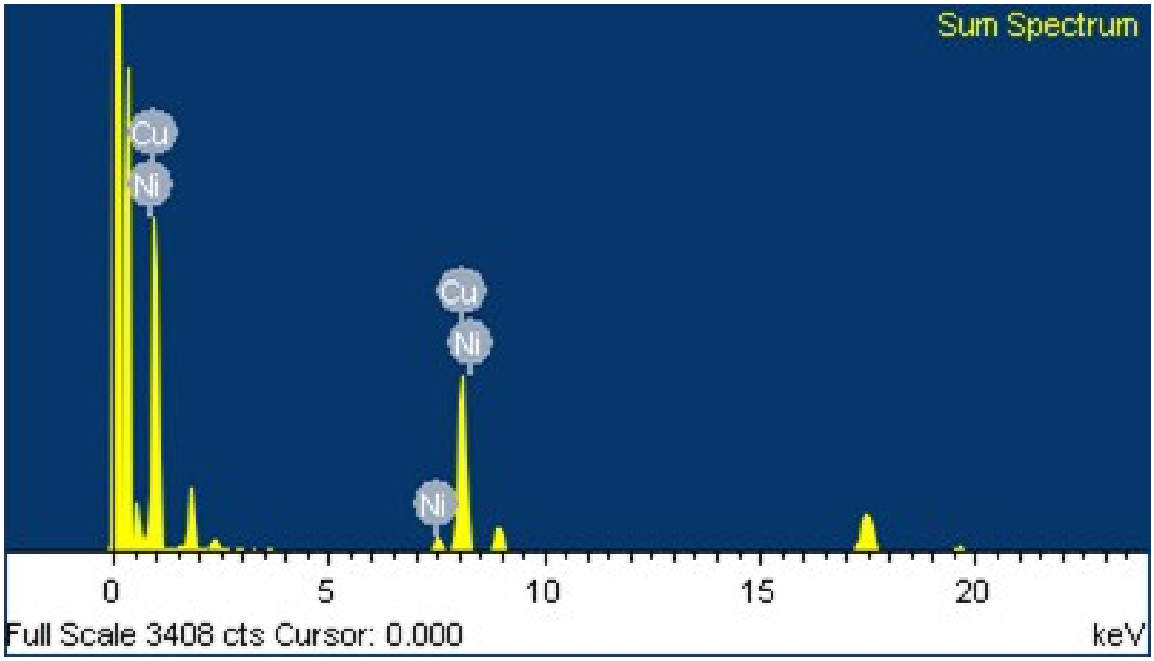

Fig. S5 The EDS spectrum of CuNi alloy NWs.

Table S1. The ratio of Cu and Ni elements for CuNi alloy NWs.

Element	Weight%	Atomic%
Ni	6.34	6.82
Cu	93.66	93.18
Totals	100.00	100.00

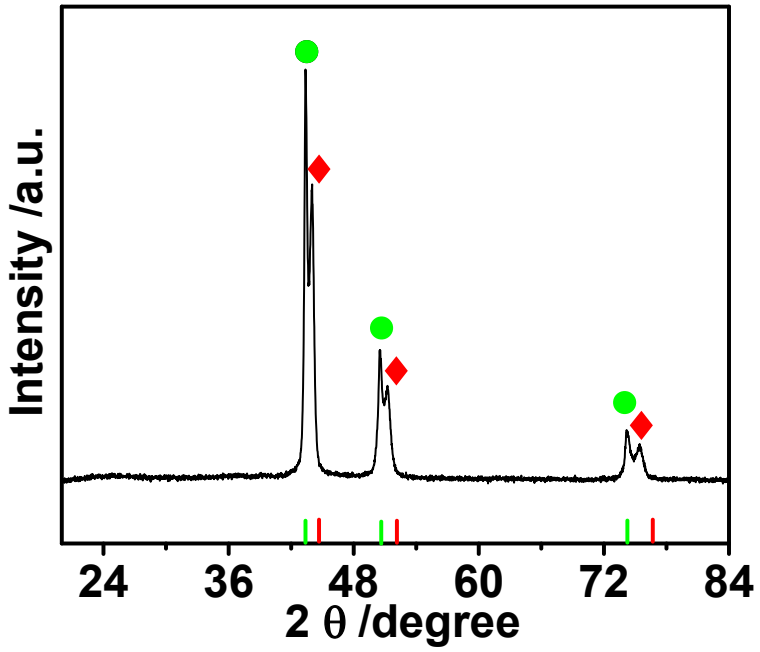

Fig. S6 The XRD of CuNi alloy NWs (the green mark is the peak of copper and red mark is corresponding to the peak of CuNi alloy).

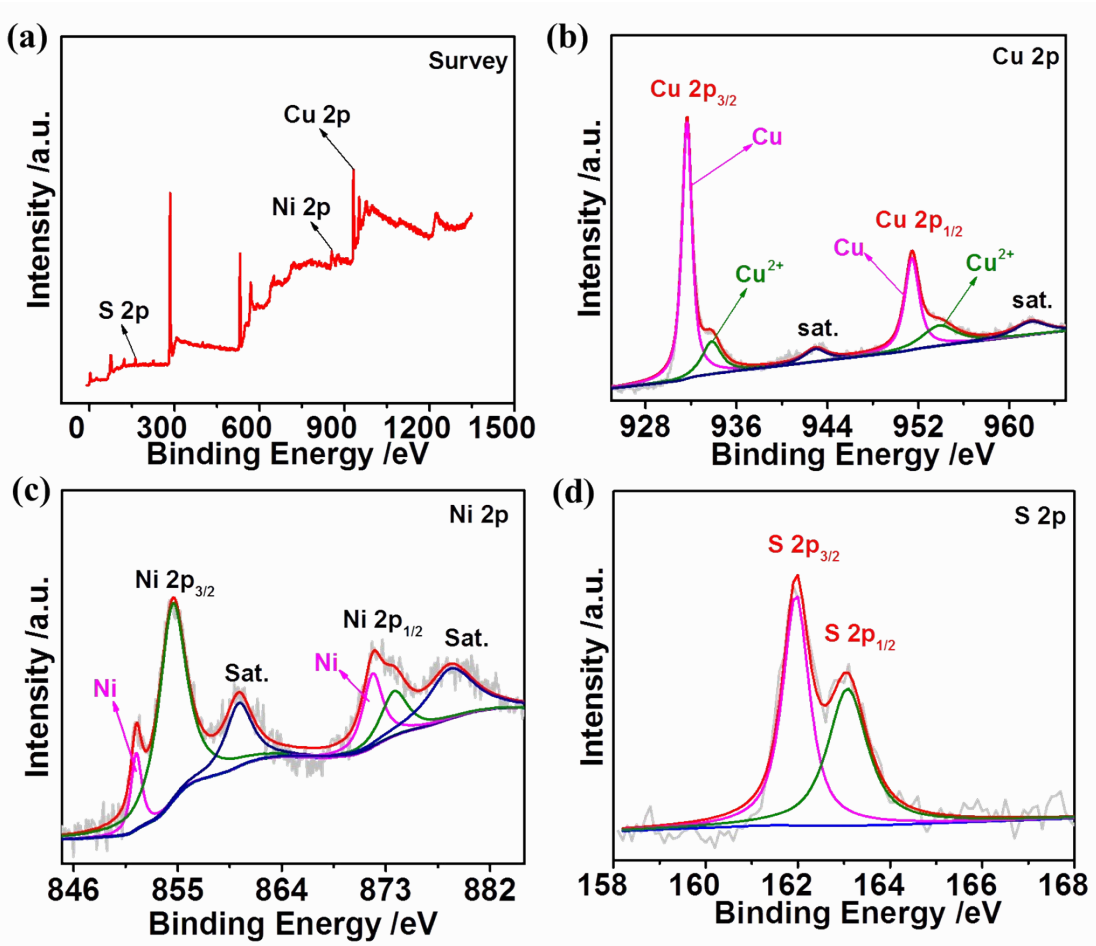

Fig. S7 (a) XPS survey spectra of copper-nickel sulfide nanowires. (b-d) illustrating the XPS spectra of Cu 2p, Ni 2p and S 2p for copper-nickel sulfide nanowires, respectively.

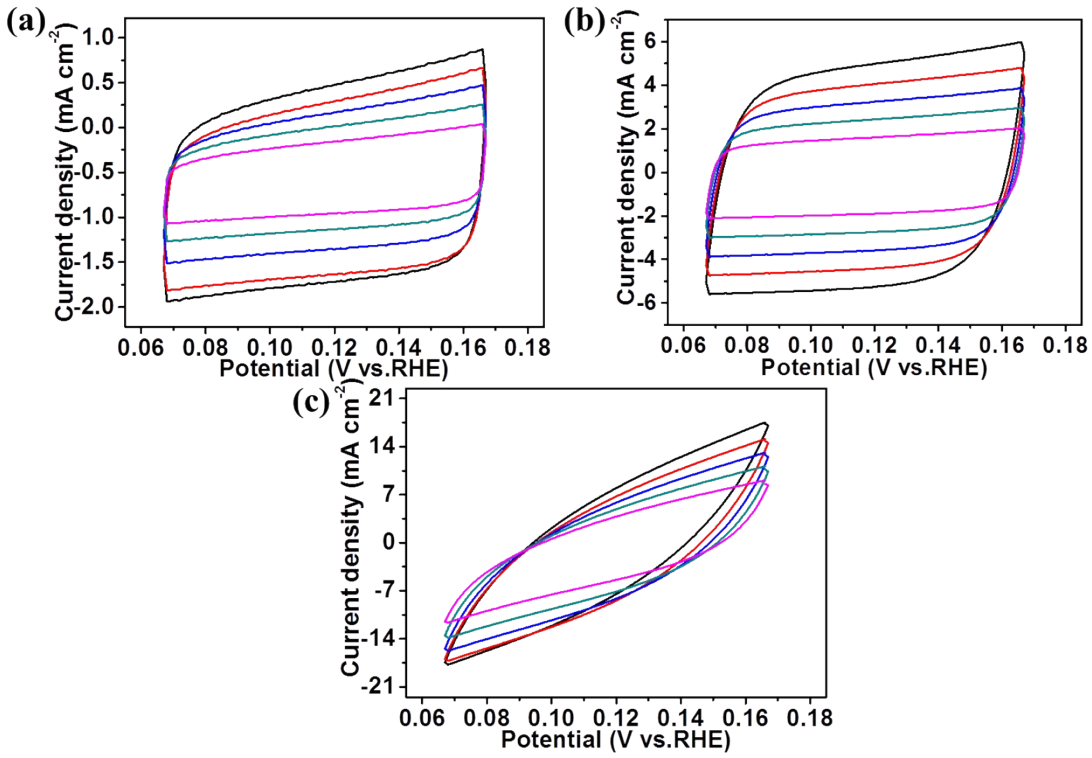

Fig. S8 Double layer capacitance measurements for HER with scan rates from 20 to 100 mV s^{-1} for (a) Cu NWs, (b) CuNi alloy NWs, and (c) copper-nickel sulfide NWs.

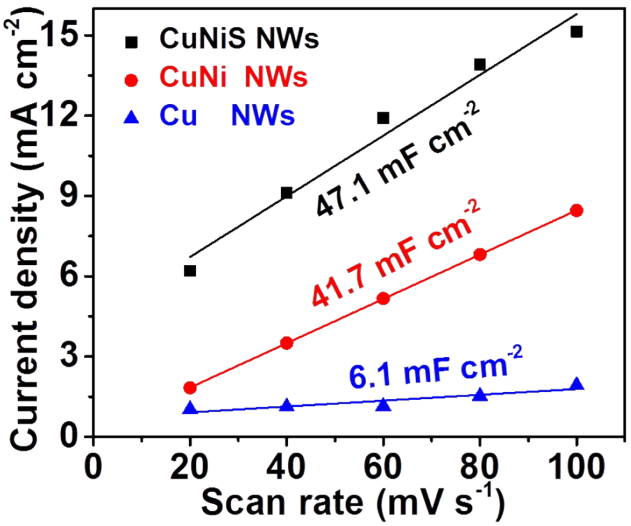

Fig. S9 Linear fitting of the capacitive currents of different catalysts versus scan rates for HER (copper-nickel sulfide nanowires are abbreviated to CuNiS NWs).

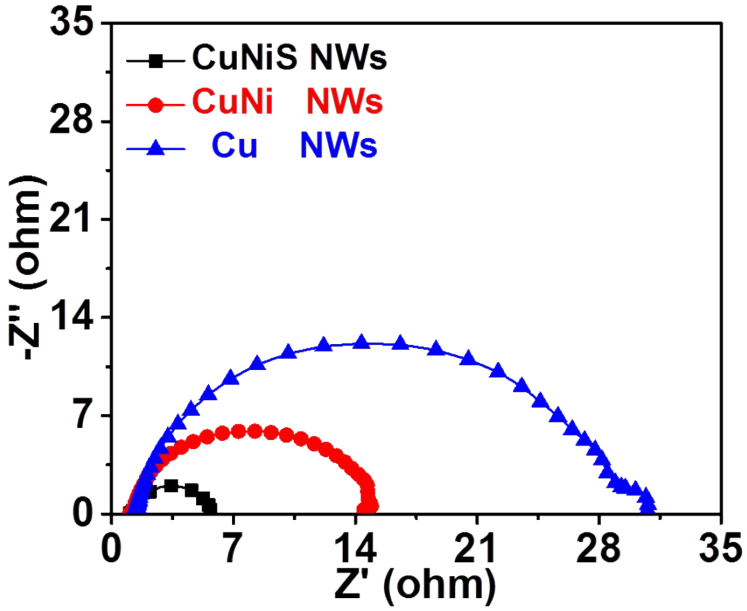

Fig. S10 The EIS Nyquist plots of different materials for HER.

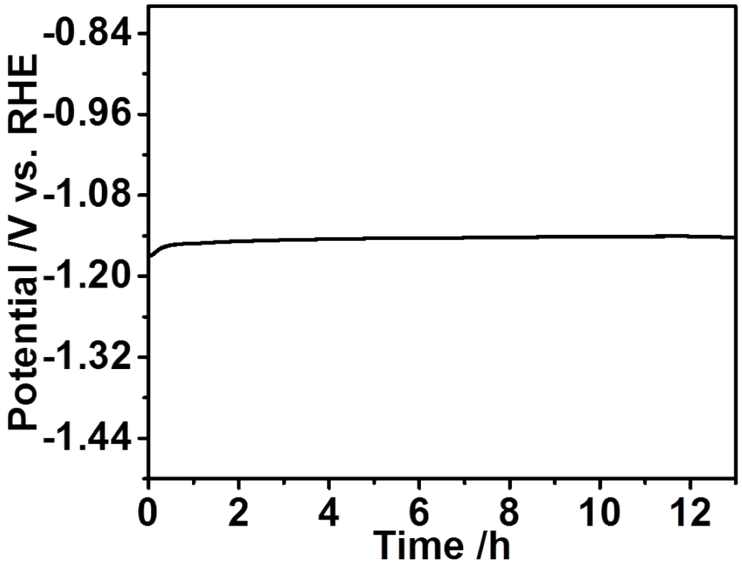

Fig. S11 Chronopotentiometric curves of copper-nickel sulfide nanowires for HER at constant current densities of 10 mA cm^{-2} in 1 M KOH.

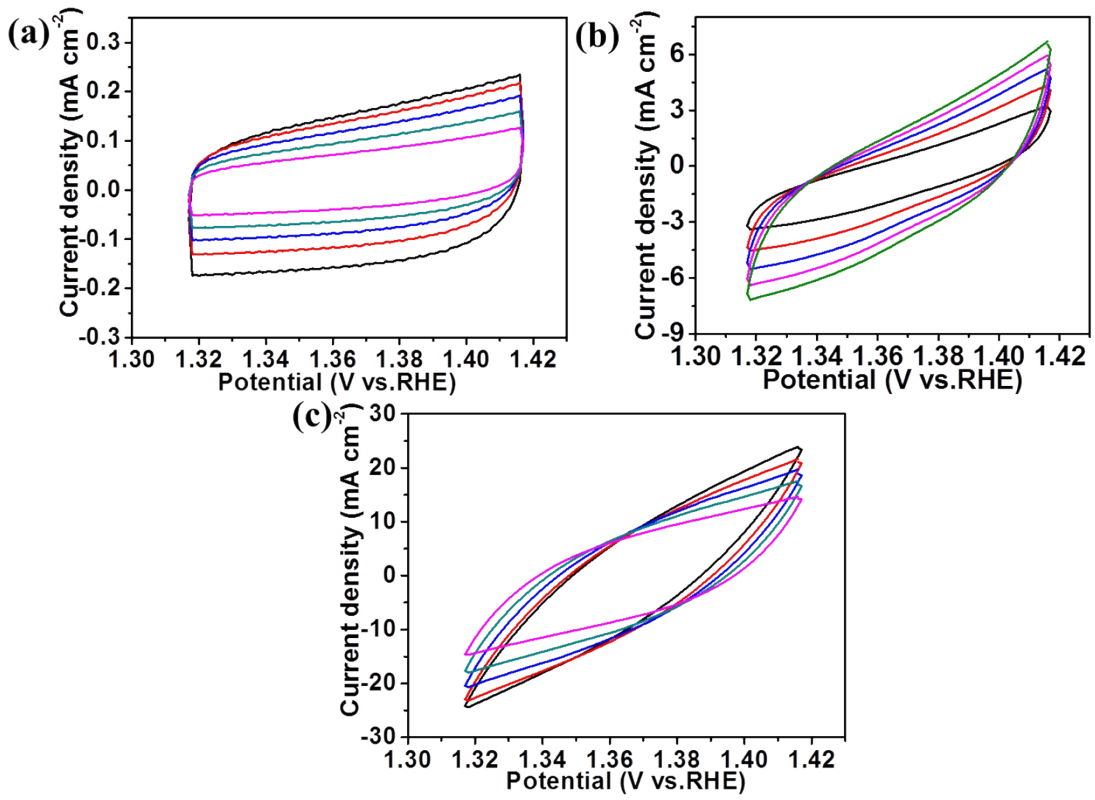

Fig. S12 Double layer capacitance measurements for OER with scan rates from 20 to 100 mV s^{-1} for (a) Cu NWs, (b) CuNi alloy NWs, and (c) copper-nickel sulfide NWs.

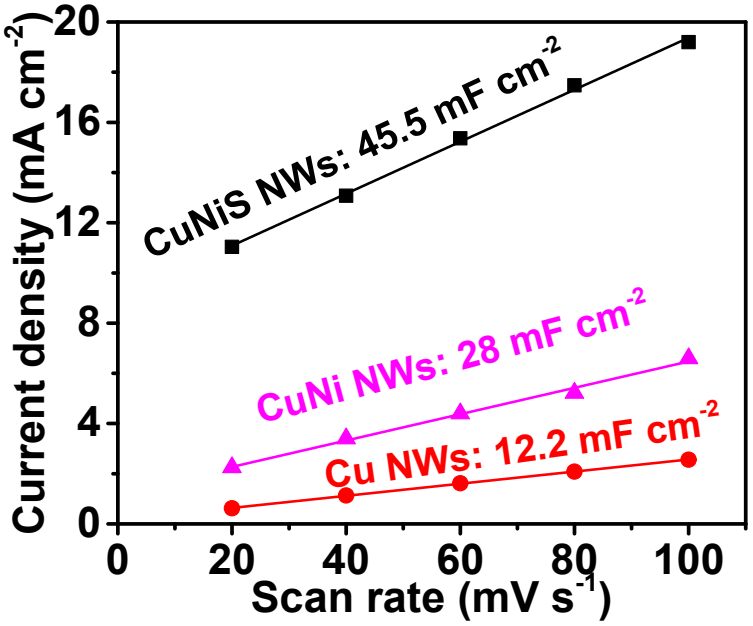

Fig. S13 Linear fitting of the capacitive currents of different catalysts versus scan rates for OER.

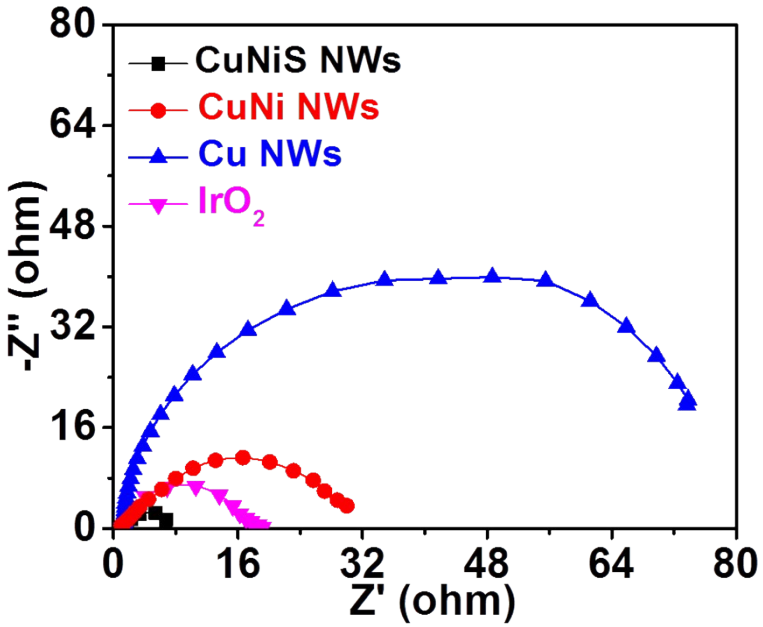

Fig. S14 The EIS Nyquist plots of different materials for OER.

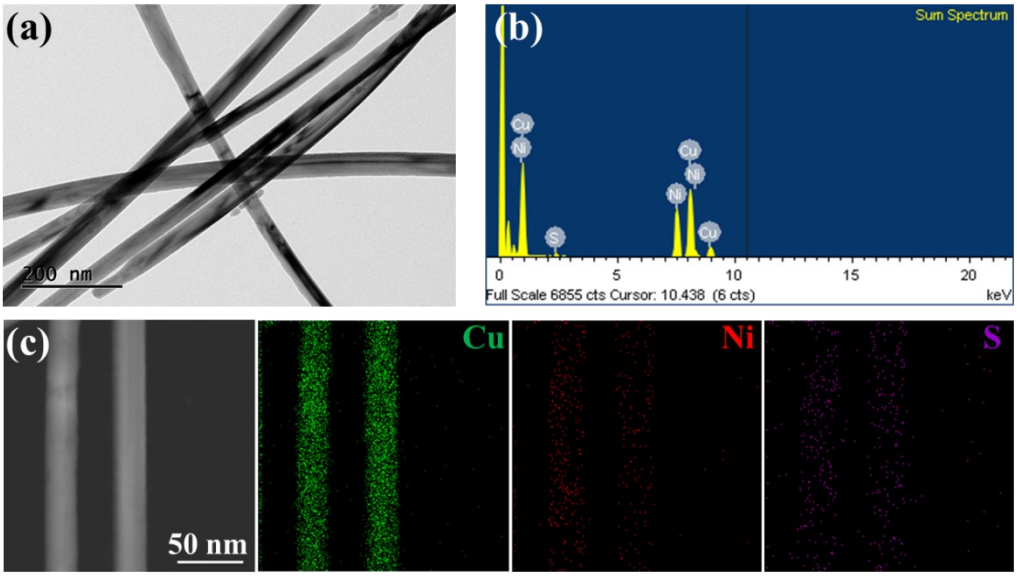

Fig. S15 (a) TEM image of copper-nickel sulfide NWs when 0.05 mmol S powder was used. (b) EDS result of copper-nickel sulfide NWs and corresponding atom ratio of Cu/Ni/S is 94.07/3.47/2.46. (c) Corresponding elemental mapping of copper-nickel sulfide NWs.

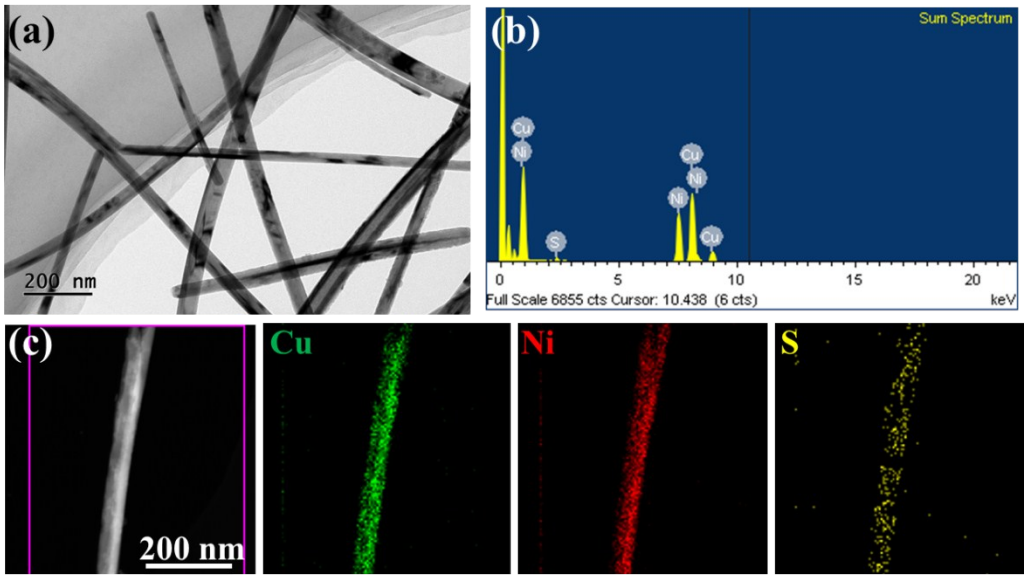

Fig. S16 (a) TEM image of copper-nickel sulfide NWs when 0.15 mmol S powder was used. (b) EDS result of copper-nickel sulfide NWs and corresponding atom ratio of Cu/Ni/S is 78.44/14.21/7.35. (c) Corresponding elemental mapping of copper-nickel sulfide NWs.

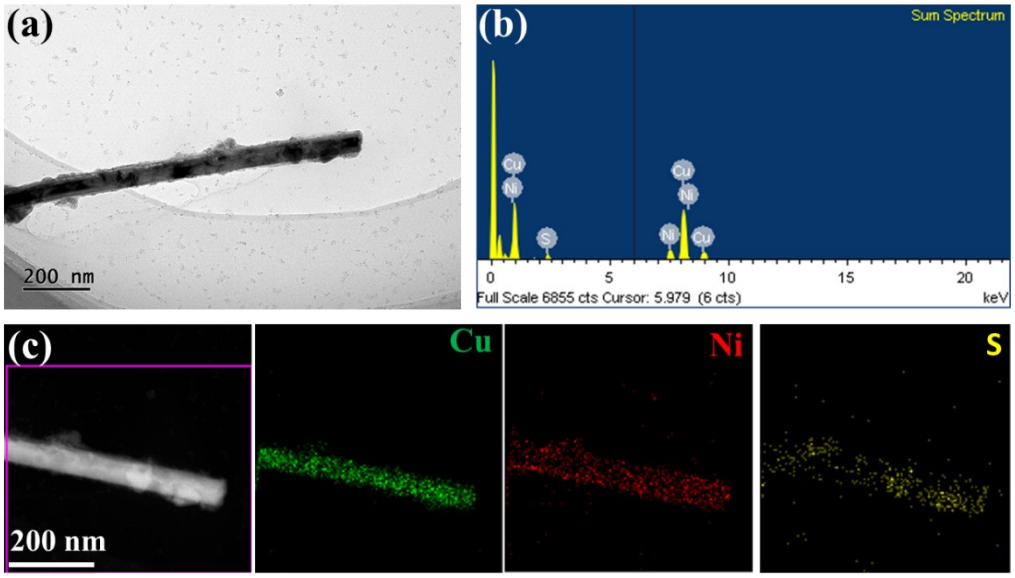

Fig. S17 (a) TEM image of copper-nickel sulfide NWs when 0.35 mmol S powder was used and obvious nanoparticles can be generated outside the nanowires. (b) EDS result of copper-nickel sulfide NWs and corresponding atom ratio of Cu/Ni/S is 59.62/30.05/10.33. (c) Corresponding elemental mapping of copper-nickel sulfide NWs.

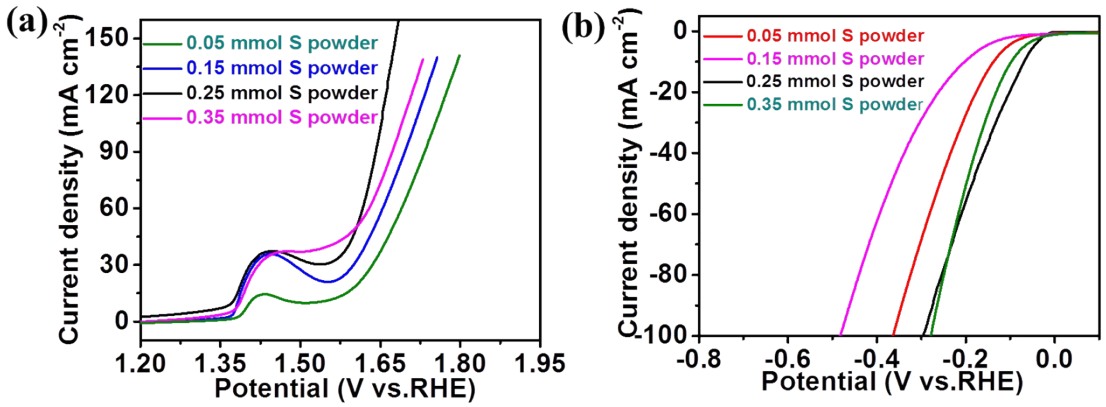

Fig. S18 The OER and HER performances for copper-nickel sulfide NWs synthesized by different amount of S powder.

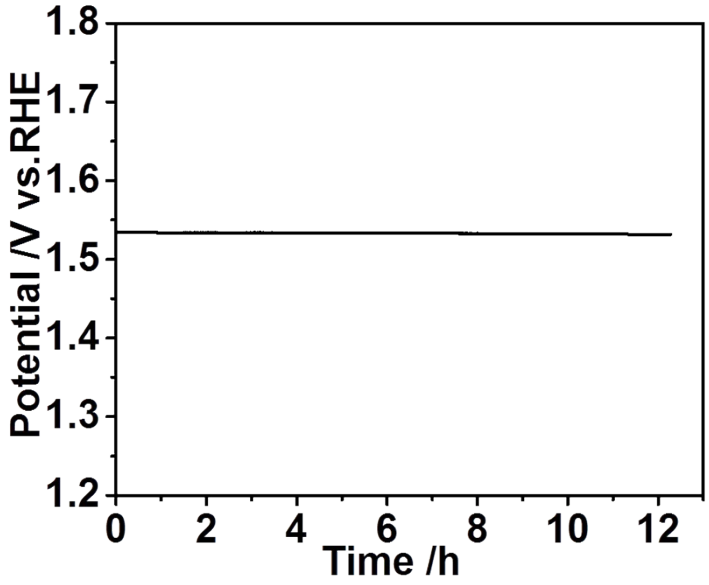

Fig. S19 Chronopotentiometric curves for copper-nickel sulfide nanowires for OER at constant current densities of 30 mA cm^{-2} in 1 M KOH.

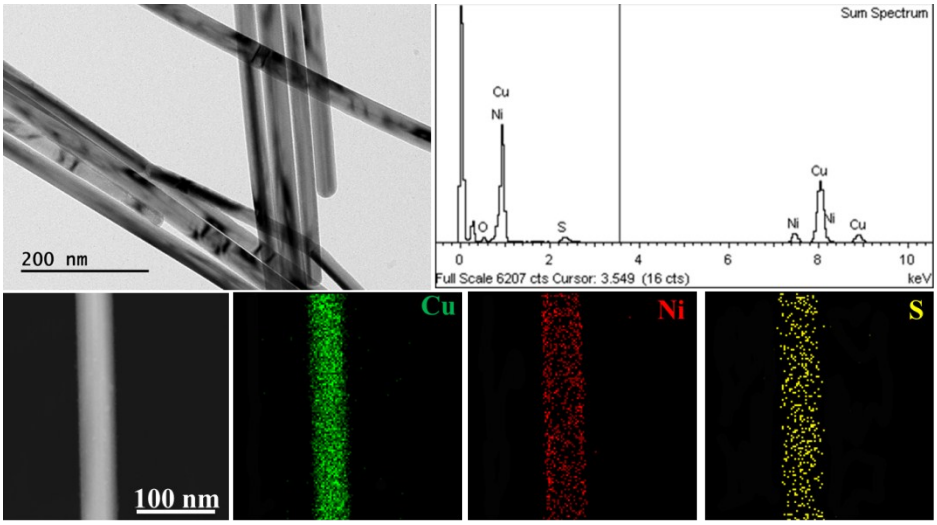

Fig. S20 (a) TEM image of copper-nickel sulfide NWs after electrochemical measurement. (b) EDS result of copper-nickel sulfide NWs. (c) Corresponding elemental mapping of copper-nickel sulfide NWs after electrochemical test.

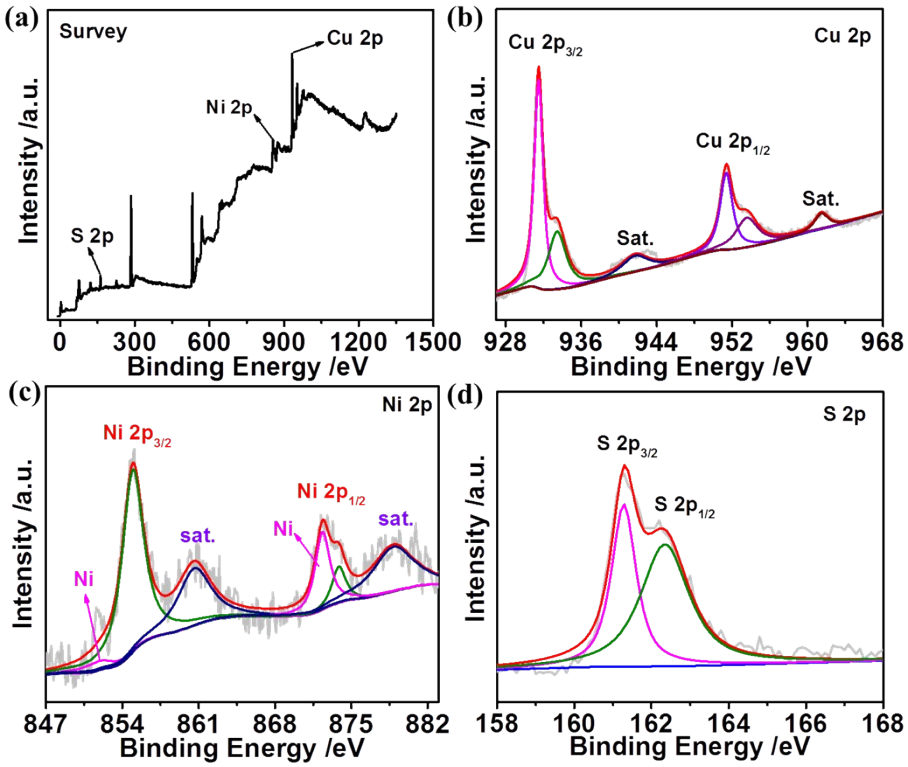

Fig. S21 The XPS results of copper-nickel sulfide nanowires after electrochemical test in 1M KOH medium.

Table S2. Comparison of HER performance of various nonprecious catalysts in alkaline medium

Catalyst	Electrolyte Solution	Current Density (mA cm^{-2})	Overpotential (mV)	References
CuNiS NWs	1M KOH	10	71	This work
CdS/Ni_3S_2/PNF	1M KOH	10	121	[1]
Co_2P/CNTs	1M KOH	10	132	[2]
Ni@NC-800	1M KOH	10	70	[3]
$Co(S_{0.71}Se_{0.29})_2$	1M KOH	10	122	[4]
$Cu_xNi_{4-x}N$/NF	1M KOH	10	12	[5]
NiS_2	1M KOH	10	148	[6]
V-Co_4N	1M KOH	10	37	[7]
Ni-Co-P	1M KOH	10	58	[8]
Ni-Co-P/NF	1M KOH	10	156	[9]
NiFe HNSs	1M KOH	10	189	[10]
Ni/V_2O_3	1M KOH	10	61	[11]

Table S3. Comparison of OER performance of various nonprecious catalysts in alkaline medium

Catalyst	Electrolyte Solution	Current Density (mA cm^{-2})	Overpotential (mV)	References
CuNiS NWs	1M KOH	30	307	This work
NiS@SLS	0.1M KOH	11	297	[12]
CdS/Ni_3S_2/PNF	1M KOH	10	151	[1]
Co_2P/CNTs	1M KOH	10	292	[2]
Ni@NC-800	1M KOH	10	280	[3]
Cu_2S/CF	1M KOH	20	336	[13]
$Co(S_xSe_{1-x})_2$	1M KOH	10	283	[4]
CuS-Ni_3S_2/CuNi/NF	1M KOH	100	337	[14]
NiS	1M KOH	10	320	[6]
Ni-Co-S/NF	1M KOH	40	270	[9]
NiFe HNSs	1M KOH	10	220	[10]
$CuCo_2S_4$/CF	1M KOH	60	259	[15]
α-$Co_4Fe(OH)_x$	1M KOH	10	295	[16]

Table S4. Comparison of cell voltage for overall water splitting of various nonprecious catalysts

Catalyst	Electrolyte Solution	Current Density (mA cm^{-2})	Voltage (V)	References
CuNiS NWs	1M KOH	10	1.54	This work
NiS // NiS_2	1M KOH	10	1.58	6
FeB_2-NF	1M KOH	10	1.57	17
Ni/Mo_2C-PC	1M KOH	10	1.66	18
Co_9S_8@NOSC-900	1M KOH	10	1.60	19
Ni@NC-800/NF	1M KOH	10	1.60	3
Co_2P/CNT	1M KOH	10	1.53	2
CdS/Ni_3S_2/PNF	1M KOH	-	1.50	1
$NiCo_2O_4$ // $Ni_{0.33}Co_{0.67}S_2$	1M KOH	5	1.65	20
np-$(Co_{0.52}Fe_{0.48})_2P$	1M KOH	10	1.53	21

1. S. Qu, J. Huang, J. Yu, G. Chen, W. Hu, M. Yin, R. Zhang, S. Chu and C. Li, *ACS Appl. Mater. Interfaces*, 2017, **9**, 29660-29668.
2. D. D and K. K. N, *Nano Energy*, 2016, **30**, 303-311.
3. Y. Xu, W. Tu, B. Zhang, S. Yin, Y. Huang, M. Kraft and R. Xu, *Adv. Mater.*, 2017, **29**, 1605957.
4. F. L, W. X. Li, Y. X. Guan, Y. Y. Feng, H. J. Zhang, S. L. Wang and W. Yu, *Adv. Funct. Mater.*, 2017, **27**, 1701008.
5. Y. M. Ma, D. H. Zheng, Z. F. Wu, B. Zhang, Y. Zhang, C. H. Xiao and S. J. Ding, *J. Mater. Chem. A,*, 2017, **5**, 24850-24858.
6. P. Luo, H. J. Zhang, L. Liu, Y. Zhang, J. Deng, C. H. Xu, N. Hu and Y. Wang, *ACS Appl. Mater. Interfaces*, 2017, **9**, 2500-2508.
7. Z. Y. Chen, Y. Song, J. Y. Cai, X. S. Zheng, D. D. Han, Y. S. Wu, Y. P. Zang, S. W. Niu, X. J. Liu and G. M. Wang, *Angew. Chem. Int. Edit.*, 2018, **57**, 5076-5080.
8. Z. W. Fang, L. L. Peng, M. Q. Y, Y., X. Zhang, Y. J. Xie, J. J. Cha and G. H. Yu, *J. Am. Chem. Soc.*, 2018, **140**, 5241-5247.
9. Y. Q. Gong, Z. F. Xu, H. L. Pan, Y. Lin, Z. Yang and J. L. Wang, *J. Mater. Chem. A*, 2018, **6**, 12506-12514.
10. X. H. Sun, Q. Shao, Y. C. Pi, J. Guo and X. Q. Huang, *J. Mater. Chem. A*, 2017, **5**, 7769-7775.
11. M. Ming, Y. L. Ma, Y. Zhang, L. B. Huang, L. Zhao, Y. Y. Chen, X. Zhang, G. Y. Fan and J. S. Hu, *J. Mater. Chem. A*, 2018, **6**, 21452-21457.
12. J. S. Chen, J. W. Ren, M. Shalom, T. Fellinger and M. Antonietti, *ACS Appl. Mater. Interfaces*, 2016, **8**, 5509-5516.
13. L. B. He, D. Zhou, Y. Lin, R. X. Ge, X. D. Hou, X. P. Sun and C. B. Zheng, *ACS Catal.*, 2018, **8**, 3859-3864.
14. N. Zhang, Y. Gao, Y. H. Mei, J. Liu, W. Y. Song and Y. Yu, *Inorg. Chem. Front*, 2018, **6**, 293-302.
15. L. Yang, L. S. Xie, X. Ren, Z. Q. Wang, Z. A. Liu, G. Du, A. M. Asiri, Y. D. Yao and X. P. Sun, *Chem. Commun.*, 2018, **54**, 78-81.
16. H. Y. Jin, S. J. Mao, G. P. Zhan, F. Xu, X. B. Bao and Y. Wang, *J. Mater. Chem. A*, 2016, **5**, 1078-1084.
17. H. Li, P. Wen, Q. Li, C. C. Dun, J. H. Xing, C. Lu, S. Adhikari, J. Lin, D. L. Carroll and S. M. Geyer, *Adv. Energy Mater.*, 2017, **7**, 1700513-1700524.
18. Z. Y. Yu, Y. Duan, M. R. Gao, C. C. Lang, Y. R. Zheng and S. H. Yu, *Chem. Sci.*, 2017, **8**, 968-973.
19. S. H. Huang, Y. Y. Meng, S. M. He, A. Goswami, T. Asefa and M. M. Wu, *Adv. Funct. Mater.*, 2017, **27**, 1606585-1606594.
20. Z. Peng, D. S. Jia, A. M. Al-Enizi, A. A. Elzatahry and G. F. Zheng, *Adv. Energy Mater.*, **5**, 1402031-1402037.
21. Y. W. Tan, H. Wang, P. Liu, Y. H. Shen, C. Cheng, A. Hirata, T. Fujita, Z. Tang and M. W. Chen, *Energy Environ. Sci.*, 2016, **9**, 2257-2261.